Electrical studies on H-implanted silicon

M. Bruni, D. Bisero, R. Tonini, and G. Ottaviani
Dipartimento di Fisica, Università di Modena, Italy

G. Queirolo and R. Bottini
SGS-Thomson Microelectronics, Agrate Brianza, Milano, Italy
(Received 13 August 1993)

Electrical properties of high-dose (1.6×10^{16} at./cm^2) H^+-implanted B-doped silicon have been investigated using transient capacitance spectroscopy, capacitance-voltage, and spreading resistance profiling. The role of hydrogen is twofold: to interact with the defects created by ion implantation, modifying their electrical properties, and to neutralize the shallow-acceptor dopants. The evolution of the defects responsible for the deep levels and the depth of the neutralized region have been investigated after isochronal annealing at various temperatures up to 800 °C. Deep-level transient spectroscopy spectra show three hole traps; two of them, H(0.67), H(0.33), have been tentatively identified as vacancy-hydrogen complexes (VH_2, VH_3) while the attribution of the third, H(0.23), detected in the samples annealed at 400–450 °C, is uncertain. As a function of the heat treatment, the total number of defects is strongly reduced at 300 °C, it increases for $T > 300$ °C and at the highest temperatures, namely 800 °C, the defects disappear. The first decrease is attributed to the formation of neutral VH_4 complexes and the disappearance to complete decoration of point defects or their agglomeration. The thickness of the passivated region has a minimum at 300 °C, which corresponds to the formation of the stable VH_4. At lower temperatures, the hydrogen necessary for the passivation is the unbonded one and presumably comes from the implantation process itself. At higher temperature, H comes from the breaking of the VH_4 or H_n complexes. These results are in good agreement with our previous studies concerning the role played by hydrogen in affecting the crystal properties of silicon.

I. INTRODUCTION

Implantation of light ions introduces defect states into the energy gap of silicon. The primary point defects, produced by the slowing down of the ion, diffuse and react to form complexes with impurity atoms or other defects.[1] It is important to distinguish between the role of the bombardment itself and that of the implanted ion species, because both contribute to defects formation. The former is present irrespective of the energy-transfer mechanism, as illustrated by the fact that the first studies of vacancy-related defects were conducted with electron- and γ-irradiated silicon. The latter is fundamental as far as hydrogen is concerned because hydrogen is a major reactant with solids due to its high chemical activity and lattice mobility. Its interactions with defects[2–6] and dopants[7–10] cause strong changes in the electrical and optical properties of crystalline silicon. Even though the structure of the hydrogen-related defects is not yet clear many studies have contributed to the knowledge of the microscopic nature of the acceptor-H complex.[10–15]

This paper is a continuation of ongoing work which has been devoted mostly to investigating the structure and metallurgical properties of single-crystal silicon heavily implanted with hydrogen.[16] The results indicate that in the region from the sample surface down to 120 nm (the hydrogen projected range is 200 nm) the initial self-interstitial distribution remains unchanged after treatments at $T \leq 300$ °C, and is appreciably annealed at 400 °C. The presence of hydrogen induces a displacement of the silicon atoms from the regular lattice; the total number of displaced atoms first increases up to 400 °C and then decreases. This behavior is attributed to the presence of hydrogen-related complexes, whose natures change with annealing conditions, rather than to the loss of hydrogen itself. Two kinds of hydrogen-related complexes are identified as sources of displacement: one (referred to as H_*), responsible for a weak displacement field, is formed in the defect-free wing of the distribution (centered on a depth of about 230 nm) and disappears after annealing at $T > 200$ °C; and the other (referred to as H_{**}), responsible for a strong displacement field, is formed in the defective region of maximum hydrogen concentration after heat treatments at $T > 200$ °C and is stable up to at least 600 °C.

In this paper we report on investigations of defects, measured by deep-level transient spectroscopy (DLTS), in *p*-doped crystalline silicon bombarded with high doses of H^+.

Sections II and III are devoted to the preparation of samples, the measurement techniques, and the results obtained.

Section IV is divided into two subsections. Section IV A deals with the dependence of the amplitude of the passivated region (x_0) on temperature. The presence of a maximum x_0 for $T = 400$ °C is explained by a model that supposes the existence of surface H reservoirs, where hydrogen is embodied in complexes of the kind defect-H, stable up to 400 °C. This idea is supported by previously quoted results[16] that show a maximum displacement field

for the same temperature.

In Sec. IV B, the deep levels observed by DLTS and their tentative identification are discussed. The defects' evolution with temperature is analyzed, and an explanation of the dependence on temperature of the relative defect concentration, which shows a minimum for $T=300\,^{\circ}\mathrm{C}$ and increases for higher temperatures, is naturally integrated into the model of Sec. IV A.

The Appendix is an attempt to answer the fundamental question: why are we able to detect deep levels? This is not a silly question. In fact, the levels we observe are associated with defects that are very close to the surface (some thousands of Å). DLTS on our samples should not give any signal corresponding to these depths, for reasons discussed below. If we depart from the DLTS standard theory and, in particular, from the depletion approximation, the electrical properties of our devices can be explained. We propose a model which accounts for the influence of the Debye carrier distribution tails on DLTS spectra of highly compensated semiconductors. In these conditions, in fact, it is not correct to assume that the space-charge region of the Al-Si junction has no free carriers when reverse biased. This neglects the presence of a transition zone, that is wide in the particular case studied, starting from the internal edge of the depleted region.

II. EXPERIMENT

Samples were prepared by implanting H_2^+ into single-crystal silicon. The silicon slices were 6-in. diameter, Czochralski grown, (100) oriented, and p type (B doped), with a resistivity in the range 3–5 Ω cm.

Samples were implanted with H_2^+ at an energy of 31 keV, and a dose of 8×10^{15} at/cm^2. Because of the H_2^+ fragmentation at the surface, this implantation is equivalent to the implantation of atomic hydrogen at double fluence and an energy of 15.5 keV.

The implantation was carried out at room temperature, by tilting the slices 7° with respect to the beam, in an Eaton Nova 10/160 ion implanter, operating at a beam-current density for which there is no appreciable sample heating.

Isochronal annealing experiments were carried out by treating the samples in vacuum in the temperature range 100–800 °C.

After annealing, aluminum contacts (0.2 μm thick) were evaporated over the implanted wafer's surface to produce rectifying devices suitable for capacitance transient analysis. Some samples, mostly the ones treated at temperatures higher than 400 °C, were heated again at 400 °C for 20 min to stabilize the contacts' properties.

The samples were characterized by capacitance-voltage (C-V) profiling, spreading resistance (SR) and deep level transient spectroscopy (DLTS). For the purposes of our research, C-V profiling and DLTS can be considered two complementary techniques: the first, in fact, is very sensitive to shallow dopants concentration, while the latter is able to detect very low concentrations of deep levels. Profiles of dopant atoms were obtained from C-V measurements by the equation

$$N(x_d)=-\frac{C^3}{e\varepsilon\varepsilon_0 A^2}\left[\frac{\Delta C}{\Delta V}\right]^{-1},\quad \text{with } x_d=\frac{\varepsilon\varepsilon_0 A}{C},$$

where ε and ε_0 are the silicon and the vacuum dielectric constants, respectively, e is the electron charge, A is the device's area, and x_d is the amplitude of the space-charge region. It should be noted that C-V analysis is not able to give information about the dopant's concentration in the region between the surface and some micrometers in depth. The minimum distance from the surface at which a differential capacitance measurement can give information is about $3L_D$,[17] where L_D is the Debye length:

$$L_D=\left[\frac{\varepsilon\varepsilon_0 kT}{e^2 N_A}\right]^{1/2}.$$

This general statement suggests that the electrically active dopant concentration near the surface of our samples has a value such that the carrier's Debye length becomes of the order of micrometers. This can be achieved only if the active boron concentration is about 10^{13} cm^{-3}.

The spreading resistance measurements were performed with a SSM-150 instrument. The samples were lapped at angles in the range between 1° and 3°. Contacts were made with two tungsten-rhodium tips, separated by a distance of 100 μm.

The DLTS experiments were carried out using a standard experimental apparatus as described by Lang,[18] the Polaron S4600, working in the scanning temperature mode ($100<T<400$ K). The sample cryostat uses a horizontal, continuous-flow, liquid-nitrogen design. The cryostat is normally evacuated to remove moisture which may interfere with the measurement. The sample is mounted using an electrical insulator (mica) together with thermal conduction paste on a metal stage. A platinum resistance thermometer and heating elements are attached directly to the stage.

Filling pulses (+0.5 V) were applied on quiescent reverse bias (−0.5 V) to produce capacitance transients. The capacitance meter was a Boonton 72b, operating with a 100-mV test signal and a 1-MHz frequency. Energy levels within the gap, due to carrier traps, were determined from Kissinger plot slope of $\ln(e_p/T^2)$ vs $1/kT$, where e_p is the rate window, varying in the range 4–5000 s^{-1}.

III. RESULTS

Figure 1 shows the spreading resistance profiles of samples annealed at different temperatures. No attempt was made to convert the SR profiles into carrier concentration profiles, because carrier mobility is not known in the high-SR region.

These profiles show the presence of a region, extending from the implanted surface to a depth of some micrometers, where the concentration of electrically active shallow impurities (which is inversely proportional to the SR value) is much smaller than that of the bulk. This is due to the well-known phenomenon of H dopant neutralization.[19] Similar results have been obtained with C-V measurements; in particular, the depths of the neutralized region and the bulk value of the shallow impurities are

comparable.

Figure 2 displays the maximum neutralization depth, defined as the depth at which the profile begins to deviate from the bulk's value, as a function of annealing temperature. Both SR and *C-V* data have been reported here, showing a good agreement between the two techniques in analyzing the dopant's neutralization effects. The passivated region has a maximum for samples annealed at 150 °C, decreases until 300 °C, increases again reaching a new maximum for $T = 400$ °C, and diminishes, but does

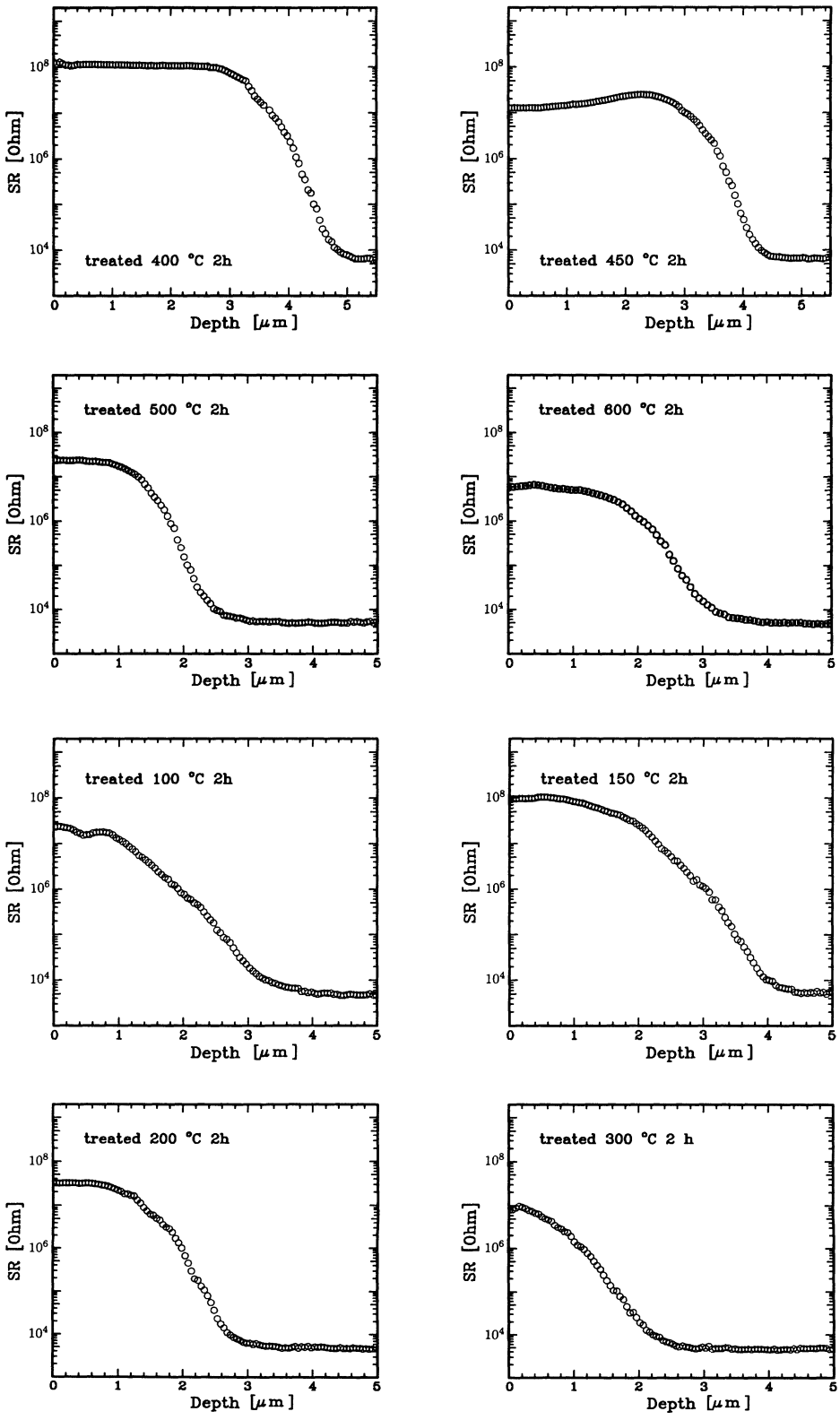

FIG. 1. Spreading resistance profiles, as a function of the annealing temperature.

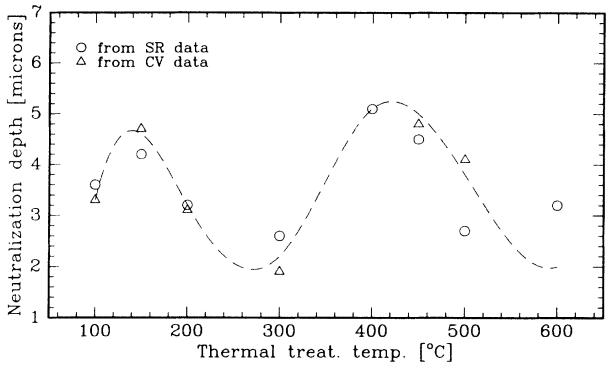

FIG. 2. Maximum neutralization depth, calculated from *C-V* and SR data, as a function of the annealing temperature.

not disappear, for temperatures up to 600 °C.

A typical DLTS spectrum obtained from an implanted sample is shown in Fig. 3. It displays a single peak (corresponding to a majority carrier trap), whose amplitude decreases exponentially with the rate window. The Kissinger[20] plot of the peak position does not exhibit a perfectly linear shape, requiring two lines instead of one. This could mean that the single peak is due to the superposition of two contributions, relating to different activation energies and capture cross sections. For this reason, we repeated the measurements with a filling pulse shorter than the former one (10^{-2} ms instead of 1 ms), in order to be able to preferentially fill the "fastest" trap. In this case, the DLTS spectrum splits into two peaks. One of them is very intense, but the other is too weak to be analyzed. The Kissinger plot relating to the strongest peak is perfectly linear (Fig. 4). Starting from this result, we tried to fit the Kissinger plot, assuming that the measured emission rate could be expressed by

$$e_p(T)=A_1T^2\exp\left[-\frac{E_1}{kT}\right]+A_2T^2\exp\left[-\frac{E_2}{kT}\right].$$

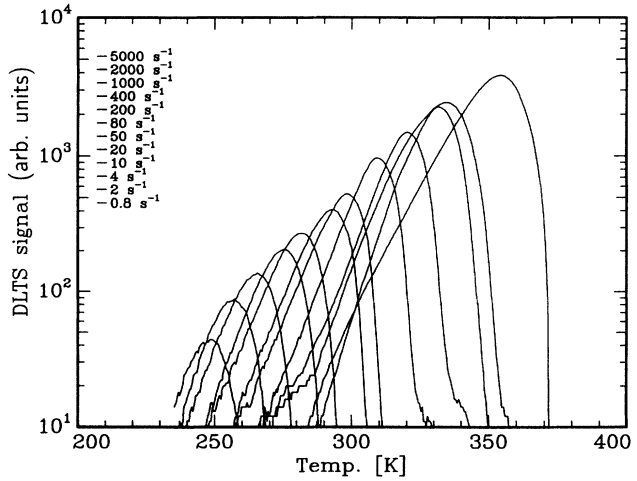

FIG. 3. The DLTS spectrum of the sample annealed for 2 h at 150 °C is shown as an example.

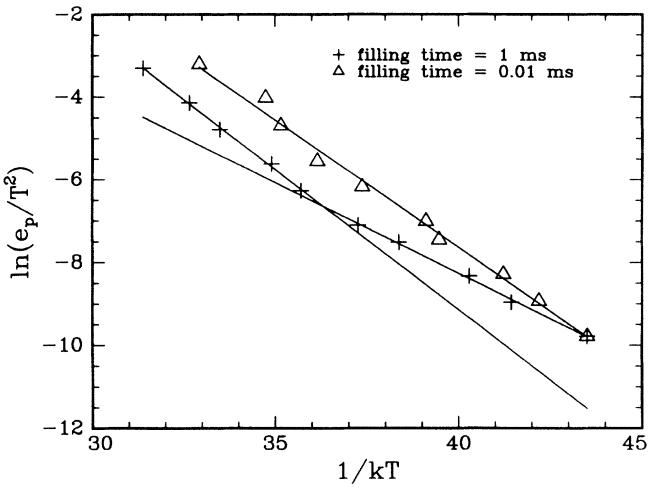

FIG. 4. Kissinger plots relative to the sample annealed at 200 °C. The crosses correspond to the DLTS measurement performed with a filling pulse of 1 ms; in this case data are fittable with two lines, because the DLTS peak comes from the superposition of two peaks. When the filling pulse is 0.01 ms the fastest trap is preferentially filled, the DLTS peak splits into two parts (one very intense and the other nearly equal to zero), and the Kissinger plot corresponding to the more intense DLTS peak is a straight line (triangles), parallel to the first part of the cross fit, that was dominated by the fastest trap. ($1/kT$ in units of eV^{-1}.)

The value E_1 has been determined from experiments to be 10^{-2} ms (note that it coincides with the value of the as implanted sample's spectrum); the preexponential factors A_1 and A_2 and the activation energy E_2 have been obtained from the fitting.

Repeating this procedure for every annealing temperature, and superimposing the corresponding Kissinger plots, we found three different groups of lines (Fig. 5). The slope of a line gives the energy level of the corre-

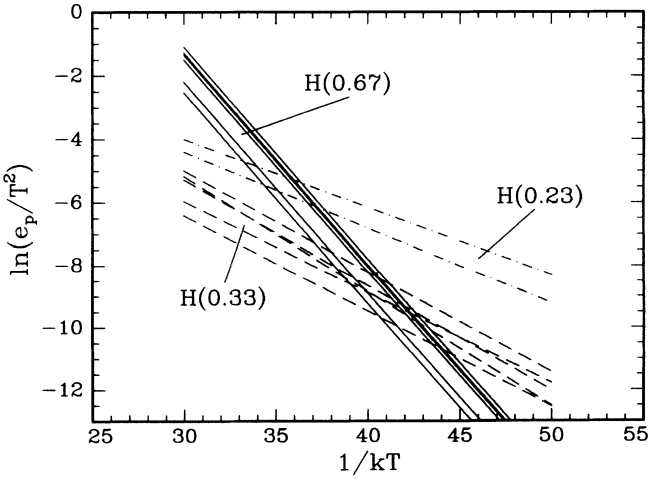

FIG. 5. Kissinger plots obtained from the fitting procedure described in the text. Three groups of lines are evident. The three corresponding defect levels are calculated as the mean value of each group. ($1/kT$ in units of eV^{-1}.)

sponding trap. We determined the average slope in each group, finding three different levels in the gap. They all correspond to majority-carrier traps (holes), and we shall refer to them hereafter as H(0.67), H(0.33), and H(0.23), making use of the standard notation H($E_t - E_v$) to indicate a hole trap with energy level E_t, ($E_t - E_v$) being the distance from the valence-band edge E_v.

Figure 6 summarizes the DLTS results, showing which are the active traps for every temperature. The values reported are the averages, calculated as described above. No values are shown for the temperature 300 °C because the signal was too weak to be analyzed.

Figure 7 shows the relative DLTS signal's amplitude corresponding to the rate window 1000 s^{-1} as a function of the sample's annealing temperature. If we suppose that the error affecting every measurement is the same, and the capture cross section varies only slightly with annealing temperature, Fig. 7 becomes a rough estimate of the relative total concentration of the traps as a function of temperature.[18] After a maximum at about 200 °C, the defects' electrical activity sharply decreases up to 300 °C, to increase again for treatments at higher temperatures.

The strong surface compensation, and the consequent high L_D value, does not allow us to obtain the trap's concentration profile,[21] as will be discussed in the Appendix. Moreover we observed that probing a region near the surface, but not including it, causes a drastic diminution of the DLTS signal that cannot be explained simply by considering the trap's refilling due to leakage currents. We can infer that the observed defects are localized near the surface, where the damage produced by hydrogen ion implantation is also present.[22] Preliminary position trapping experiments, performed in similar samples, show that traps are located a few thousand Å below the sample surface.

It seems very reasonable to associate the deep levels observed with the presence of implantation damage, which consists mainly of vacancies at our implant energy, and to their possible interaction with hydrogen atoms introduced in the crystal.

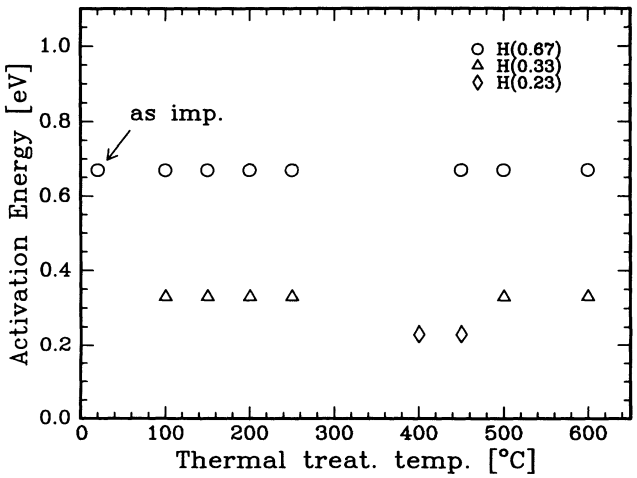

FIG. 6. Traps that are present in samples annealed at different temperatures.

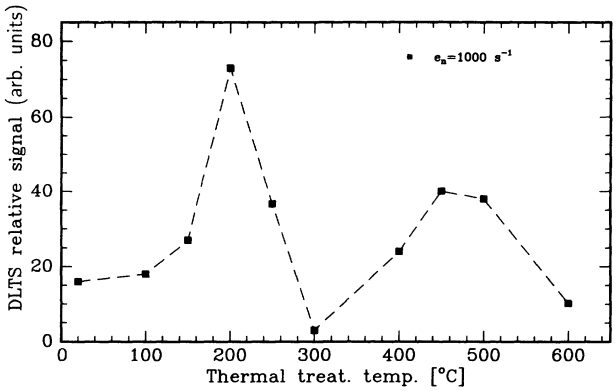

FIG. 7. Relative DLTS signal amplitude vs sample annealing temperature (rate window: 1000 s^{-1}).

IV. DISCUSSION

The experimental results show that the implantation produces defects, and the action of the hydrogen is twofold: to interact with the defects modifying their electrical properties, and to compensate for the shallow donor dopant. We recall again that *C-V* and SR techniques provide information about shallow dopant (boron) compensation processes, and DLTS explains electrical behavior of the defects created by implantation.

A. Hydrogen diffusion and dopant neutralization profiles

In Sec. III, we pointed out that the amplitude of the passivated region (x_0) decreases with temperature up to 300 °C, but displays an unexpected increasing at 400 °C. The following analysis is an attempt to explain the dependence of x_0 on T.

The secondary-ion-mass spectroscopy (SIMS) profile of the as-implanted sample, which does not exhibit substantial differences for treatments up to 400 °C, shows that the hydrogen peak concentration is about six orders of magnitude greater than the bulk boron concentration.[23] Furthermore, if we suppose the implanted dose to be distributed so that the hydrogen concentration profile becomes constant and equal to that of boron (5×10^{15} cm^{-3}), we find that the silicon wafer thickness is not enough to accommodate all the implanted H. If we consider the high diffusivity of H in silicon at room temperature and neglect the outgoing H fraction during thermal annealing, we would expect x_0 of a boron-doped silicon perfect crystal to be equal to the wafer's thickness after hydrogenation, if several features, that we shall describe in the following, did not influence the H distribution.

It is well known that the implanted hydrogen can be trapped by boron atoms and silicon dangling bonds, at temperature below 200 °C.[24] Recently it has been shown that two H complexes, called H_* and H_{**},[16] which form in implanted samples are stable in temperature. In particular, H_* is stable up to 200 °C, whereas H_{**} is stable up to higher temperatures and is present in samples annealed at 600 °C for 2 h.

For the purposes of this paper, we now define two different regions within our samples: region 1 extends

from the surface down to 0.5 μm, and region 2 starts from 0.5 μm and ends at a depth of 5 μm. The two regions are distinguished by different H concentrations and different H bonding states within the silicon lattice. We compare their main features below.

Region 1	Region 2
H conc. $\gg$ B conc.	H conc. $\sim$ B conc.
Defects conc. is very high	No defects
H is bound to:	H is bound mainly to boron atoms
(a) boron	
(b) H_* and H_{**} complexes	
(Defect-H) conc. $\gg$ (B-H) conc.	(B-H) conc. $\gg$ (defect-H) conc.

Starting from these observations we propose the following model.

When the temperature is below 150 °C, the B-H bonding is stable, and x_0 increases because of the neutralization efficiency's rise with temperature.[25]

When $200 < T < 400$ °C, the H fraction bound to boron in region 2 debonds and diffuses, while the H concentration in region 1 does not suffer any change. Thus the H atoms freed from B-H bonds of region 2 are not replaced.

For temperatures higher than 400 °C (Fig. 8), the hydrogen embodied in complexes of the kind defect-H, which can be regarded as surface H reservoirs, debonds and diffuses with a typical Gaussian profile.[26,27] At the end of the annealing process, when temperature has moved below 150 °C, the diffused H neutralizes the dopant atoms. With increasing temperature, the hydrogen Gaussian profile broadens and lowers, while its intersection with the line $y = 5 \times 10^{15}$ cm^{-3} (B concentration), which we can consider as an estimation of x_0, moves toward the sample's surface.

B. Hydrogen effect on deep levels

In Sec. III we stressed that observed deep levels could be associated with the interaction between hydrogen and the implantation damage. On the other hand, the traps we found can be due either to interfacial states produced by aluminum contact evaporation or to H-ion implantation and subsequent thermal treatments. In addition, the diodes made on unimplanted silicon show hole trap H(0.37). To discover if this level originates from interfacial states, we annealed the diode at 400 ° C for 20 min. It is well known that such a treatment removes the thin oxide layer between the metal and the semiconductor, and is strong enough to eliminate most of interfacial states.

The result of the DLTS measurement on the annealed

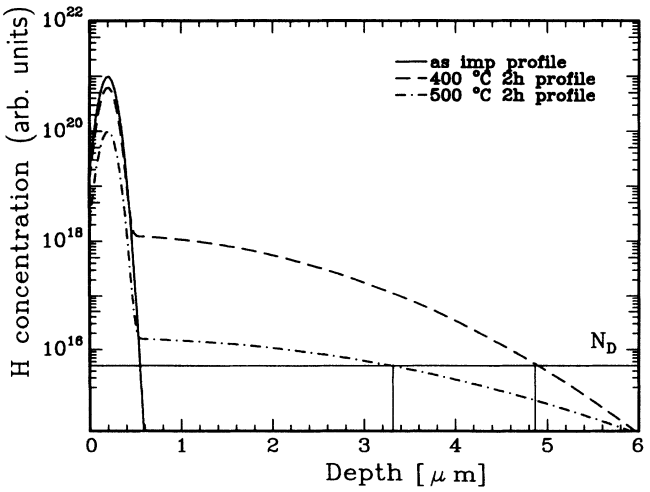

FIG. 8. Schematic view of the H-diffusion process suggested in the text, undetectable by means of analysis techniques. A portion of the hydrogen stored in the surface "reservoir" loosens and diffuses in region 2.

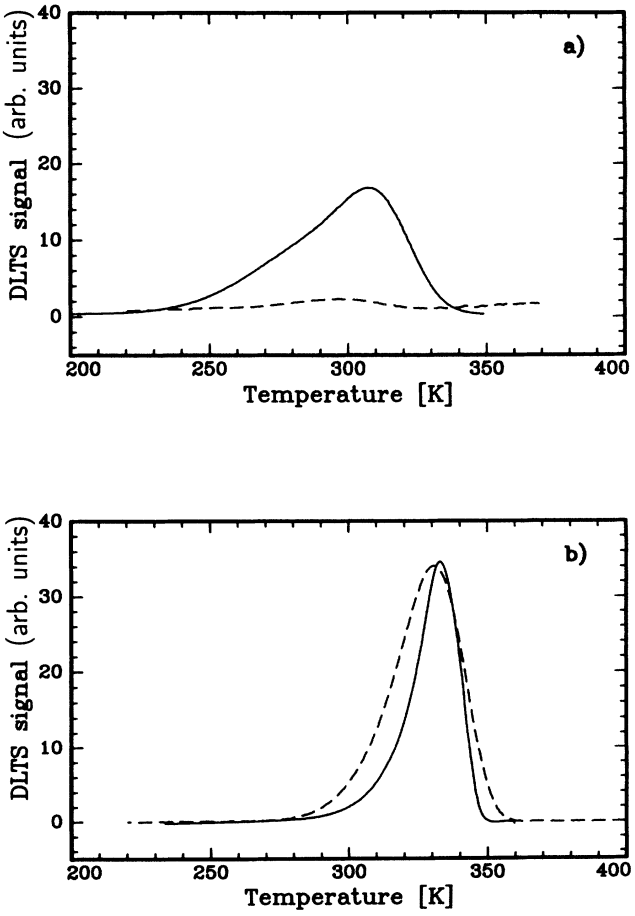

FIG. 9. DLTS spectra of the unimplanted sample (a) and of the implanted 500 °C annealed sample (b), before and after the "interfacial treatment." Solid curves and dashed curves represent unimplanted samples, and samples annealed at 400 °C for 20 min, respectively.

sample is shown in Fig. 9(a). Level H(0.37) has almost disappeared after annealing, confirming that it was due to surface states. A similar treatment was performed on H-implanted samples, previously annealed at temperatures higher than 400 °C (in samples of this kind, the "interfacial treatment" has little effect on the H distribution). In this case [Fig. 9(b)], the DLTS spectrum has not changed substantially, showing that deep levels of implanted samples are not correlated to interfacial states.

We now observe that the dependence of the relative concentration of deep levels derived from DLTS experiments on temperature, mentioned in Sec. III is very similar to the one concerning the dopant's passivation discussed in the previous paragraph. In the following we will try to correlate these two effects.

We hypothesize that the presence of deep levels is due to the interaction between vacancies produced by ion implantation and hydrogen introduced into the semiconductor. This conjecture appears to be reasonable if we observe the following.

(1) The implanted samples reveal very high concentrations of vacancies and hydrogen.

(2) The silicon dangling bonds tend to capture hydrogen atoms even when temperature is low.

(3) Deep levels associated with complexes composed of a vacancy and n ($n=1,2,3$) hydrogen atoms have been theoretically calculated.

To the best of our knowledge, none of the levels observed in the literature have been ascribed to a vacancy-H_n complex for certain, even if many reasonable attributions have been attempted.[28–31] Moreover, the number of electrical studies carried out on high fluence hydrogen-implanted silicon is too small to allow a direct comparison of literature data with our results.

From a theoretical point of view, many papers have been published concerning the calculation of energy levels related to an isolated vacancy and a vacancy decorated with one or more hydrogen atoms.[32–35] The values obtained are very different and too model dependent to be considered conclusive for deep-level identification. Nevertheless all these papers agree on two assertions.

(a) When the number n of H atoms belonging to the same vacancy increases, the electronic level associated with the complex VH_n moves toward the valence band.

(b) The completely decorated vacancy is not electrically active.

We now assume that the concentration of undecorated vacancies is negligible, because of the high H concentration, the high H mobility, and the facility of H to bind to silicon dangling bonds. Ruling out the possibility of the presence of traps due to undecorated vacancies, we tentatively attribute level H(0.67) to the complex VH_2, because of its relatively high activation energy, that could be ascribed to the binding of the two unsaturated orbitals, giving a distorted orbital, which needs an energy expense to be broken (Fig. 10).

Level H(0.33) is identified with a complex VH_n, with odd n. In fact both VH_1 and VH_3 have a single dangling bond which cannot bind with other silicon bonds. This circumstance could account for the lower energy compared with the H(0.67) center. In order to discriminate between VH_1 and VH_3, we note that this level appears after a 100 °C annealing (Fig. 6), whereas the H(0.67) level is already active in as-implanted samples; moreover, it is clear that increasing the number of H atoms requires an energy expense. Thus we identify level H(0.33) with the center VH_3.

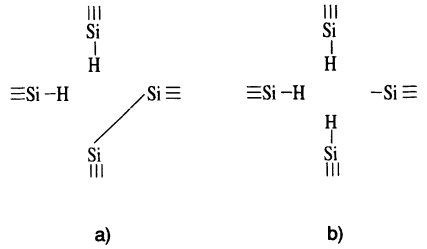

FIG. 10. Representation of a two- (a) and three- (b) hydrogen-decorated vacancy.

The origin of the lowest level H(0.23), appearing at 400 °C, is uncertain. In fact, it is very close to the level ascribed to the divacancy complex in the literature.[36] On the other hand, we observe that this level arises when the lattice displacement field is maximum.[16] Therefore, we could also attribute it to the accumulation of microscopic bubbles connected with defect clustering. This attribution would be in agreement with the general picture of the observed phenomenology.

We conclude that for thermal annealings up to 300 °C, hydrogen decorates the vacancies, forming complexes with increasing thermal stability. This gives rise to the levels H(0.67) and H(0.33), whose concentrations increase up to 250 °C. We believe that at 300 °C most vacancies are completely decorated with H atoms. Since the complex VH_4 is not electrically active, the DLTS signal drops out at this temperature. When $T \geq 400$ °C, the vacancy-hydrogen bonds begin to break (this is confirmed by C-V and SR measurements), inducing a partial vacancy depletion, which restores the VH_n electronic levels.

V. CONCLUSIONS

Defect levels of high-dose H-ion-implanted silicon were studied by transient capacitance spectroscopy, capacitance-voltage, and spreading resistance profiling. The hydrogen diffusion and the dopant's neutralization were also studied, showing that the amplitude of the passivated region decreases with temperature up to 300 °C but displays an increase at 400 °C. An interpretation of the dependence on temperature of the passivated region's amplitude was given. Three hole traps have been observed. The H(0.67) and H(0.33) levels are considered to be hydrogen related, and tentatively identified as VH_2 and VH_3 complexes, respectively. We believe that level H(0.23) could be connected with defect clustering, that is, a hydrogen-related phenomenon occurring at 400 °C. The fact that it is very close to the level ascribed to the divacancy complex in the literature makes this attribution uncertain.

ACKNOWLEDGMENT

The authors would like to thank E. Gombia, M. Capizzi, and G. F. Cerofolini for helpful discussions.

APPENDIX

CV and SR analyses have pointed out the role of H-ion implantation in the formation of a strongly compensated region lying below the crystal's surface.

We expect that if a Schottky rectifying junction is made on this material, the amplitude of the resulting space-charge region x_d must turn out to be very similar to the compensated one. In fact, for a metal-semiconductor junction, the following equation is valid:

$$x_d = \left[\frac{2\varepsilon\varepsilon_0 (V_a + V_b)}{eN_A} \right]^{1/2},$$

where V_a is the bias potential, V_b is the contact potential, e is the electron charge, and ε and ε_0 are the silicon and the vacuum dielectric constants, respectively.

If the dopant concentration N_A at the surface goes, for example, from 5×10^{15} to 5×10^{13} cm^{-3} because of the hydrogenation process (that is, the neutralization efficiency is 99%, in agreement with typical values found in B-H experiments[37]), x_d measured at zero bias must increase from 0.3 to 3 μm. Now let us consider the following statements.

(a) In general, a DLTS measurement of filling pulse V_0 cannot give any information about regions lying at a distance lower than $\lambda(V_0)$ from the surface, where λ represents the length at which the deep level E_t crosses the Fermi level.

(b) It seems to be very reasonable to suppose $\lambda > \lambda_{\text{imp}}$, where λ_{imp} indicates the amplitude of the H-implanted region, since the latter extends from the surface down to a few thousand Å.

(c) The samples which have not undergone H implantation are free from deep levels.

Taking these arguments into account, we should not be able to detect any deep level related to H-defect complexes situated in the near-surface region, and no peak should be present in our DLTS spectra.

That, in turn, means that we have to modify the standard model used for DLTS. In fact, the abrupt approximation mentioned above assumes that the space-charge region of a metal-semiconductor junction in reverse bias conditions has a carrier concentration exactly equal to zero. This hypothesis neglects the presence of a transition zone near the internal edge of the depleted region, in which the carrier distribution $p(x)$ does not change abruptly, but varies with a Gaussian law:

$$p(x) = N_A \exp\left[-\frac{(x_d - x)^2}{2L_D^2} \right].$$

If silicon is strongly compensated, L_D can be large enough to cover the whole depleted region. Therefore, it is possible that a defect far from the edge of the space-charge region is reached by a certain number of carriers belonging to the "Debye tail," as shown in Fig. 11.

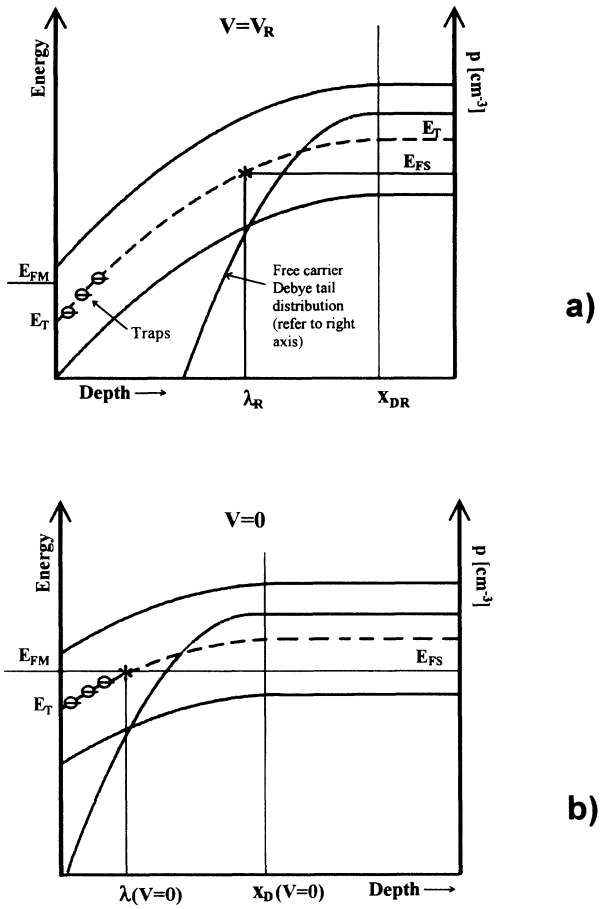

FIG. 11. Sketch of the possible filling mechanism of surface traps due to carriers belonging to the Debye tail, in a p-doped and highly passivated semiconductor. The * symbol represents a boundary point: traps on its right are filled, traps on its left are empty. Thus the traps close to the surface are not filled by the pulse at $V=0$ (b), but the Debye tail that does not reach them when $V=V_R$ (a) touches the traps at $V=0$, because of the x_D shift.

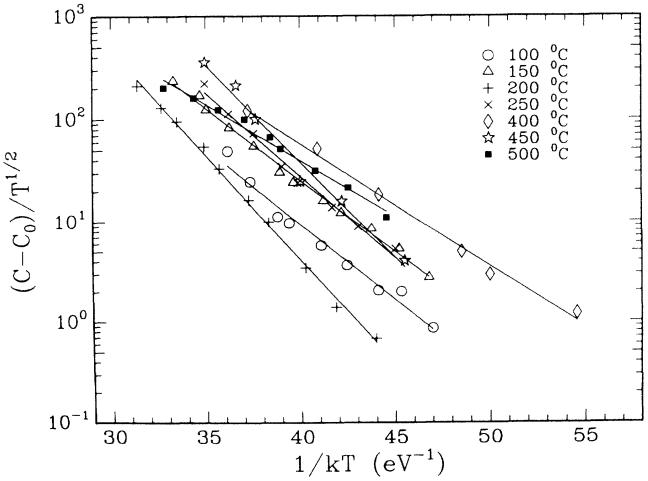

FIG. 12. Plots of the signal amplitudes, obtained from the DLTS data.

TABLE I. ξ values obtained from the equation in the text, giving a as a function of N_A (supposing $N_A = 5\times10^{13}$ cm^{-3}).

Sample	ξ
100 °C	3.0 μm
150 °C	2.9 μm
200 °C	3.5 μm
250 °C	3.1 μm
400 °C	2.7 μm
500 °C	2.6 μm

Now we try to calculate the contribution of carrier tails to the capacitance signal of a metal-semiconductor junction, containing a trap T. Let us define x_T as the trap's depth, N_T as the trap's concentration, N_{TO} as the concentration of occupied traps, c_p as the trap's capture rate, and p as the hole's concentration. We think it is reasonable to suppose $N_T(x = x_T) > p$, and thus a linear dependence of N_{TO} on p, through the hole capture cross section σ_p and the average thermal hole velocity $\langle v_p \rangle$:

$$N_{TO} \propto c_p = \sigma_p \langle v_p \rangle p \ .$$

The amplitude ΔC of the DLTS signal will be proportional to the concentration of the filled traps:

$$\Delta C \propto \sigma_p N_A \left[\frac{3kT}{m} \right]^{1/2} \exp\left[-\frac{\xi^2}{2L_D^2} \right] ,$$

where $\xi = x_d - x_t$ is the trap's distance from the space-charge region's edge. If we write the dependence on temperature, neglecting σ_p dependence, as

$$\Delta C \propto \sigma_p N_A \left[\frac{3kT}{m} \right]^{1/2} \exp\left[-\frac{\xi^2 e^2 N_A}{2kT\varepsilon\varepsilon_0} \right] ,$$

and plot $\ln(\Delta C/T^{1/2})$ vs $1/kT$ (Fig. 12),we have to find a line with slope

$$a = \frac{\xi^2 e^2 N_A}{2\varepsilon\varepsilon_0} \ .$$

In order to check the validity of the hypotheses supporting our model, it is possible to estimate the value of ξ from the former equation. This should be very similar to that of the compensated region given in Fig. 12. From the plot's slopes, assuming a dopant concentration of 5×10^{13} cm^{-3}, we have obtained ξ values shown in Table I.

These values are in good agreement with the hypothesis that deep levels are nearer to the surface than to the edge of the space-charge region. We believe this is one more confirmation of the validity of the proposed model.

[1] J. W. Corbett, J. P. Karins, and T. Y. Tan, Nucl. Instrum. Methods **182/183**, 457 (1981).
[2] S. T. Picraux and F. L. Vook, Phys. Rev. B **18**, 2066 (1978).
[3] J. Stein, Phys. Rev. Lett. **43**, 1030 (1979).
[4] T. S. Shi, S. N. Sahu, G. S. Oehrlein, A. Hiraki, and J. W. Corbett, Phys. Status Solidi A **74**, 329 (1982).
[5] B. N. Mukashev, K. H. Nussopov, M. F. Tamendarov, and V. F. Frolov, Phys. Lett. **87A**, 376 (1982).
[6] C. Dubé and J. I. Hanoka, Appl. Phys. Lett. **45**, 1135 (1984).
[7] C. T. Sah, J. Y.-C. Sun and J. J.-T. Tzou, Appl. Phys. Lett. **43**, 204 (1983).
[8] J. I. Pankove, D. E. Carlson, J. E. Berkeyheiser, and R. O. Wance, Phys. Rev. Lett. **51**, 2224 (1983).
[9] J. I. Pankove, R. O. Wance, and J. E. Berkeyheiser, Appl. Phys. Lett. **45**, 1100 (1984).
[10] N. M. Johnson, Phys. Rev. B **31**, 5525 (1985).
[11] J. I. Pankove, P. T. Zanzucchi, C. W. Magee, and G. Lucovsky, Appl. Phys. Lett. **46**, 421 (1985).
[12] M. Stavola, S. J. Pearton, J. Lopata, and W. C. Dautremont-Smith, Phys. Rev. B **37**, 8313 (1988).
[13] A. D. Marwick, G. S. Oehrlein, and N. M. Johnson, Phys. Rev. B **36**, 4539 (1987).
[14] B. Bech Nielsen, J. U. Andersen, and S. J. Pearton, Phys. Rev. Lett. **60**, 321 (1988).
[15] G. G. De Leo and W. B. Fowler, Phys. Rev. B **31**, 6861 (1985).
[16] G. F. Cerofolini, L. Meda, R. Balboni, F. Corni, S. Frabboni, G. Ottaviani, R. Tonini, M. Anderle, and R. Canteri, Phys. Rev. B **46**, 2061 (1992).
[17] P. Blood, Semicond. Sci. Technol. **1**, 7 (1986).
[18] D. V. Lang, J. Appl. Phys. **45**, 3023 (1974).
[19] R. G. Mazur and R. H. Dickey, J. Electrochem. Soc. **113**, 255 (1966).
[20] H. E. Kissinger, Anal. Chem. **29**, 1702 (1957).
[21] D. Stiévenard, M. Lannoo, and J. C. Bourgoin, Solid-State Electron **28**, 485 (1985).
[22] J. Tatarkiewicz (unpublished).
[23] L. Meda, G. F. Cerofolini, G. Ottaviani, R. Tonini, F. Corni, and R. Balboni, M. Anderle, R. Canteri, and R. Dierckx, in *Hydrogen in Semiconductors, Proceedings of the Sixth Trieste IUPAP-ICTP Semiconductor Symposium, 1990* (Ref. 22), p. 259.
[24] J. I. Pankove, in *Hydrogen in Semiconductors,* edited by J. I. Pankove and N. M. Johnson, Semiconductors and Semimetals Vol. 34 (Academic, London, 1991), p. 45.
[25] J. I. Pankove, J. Appl. Phys. **68**, 6532 (1990).
[26] J. I. Pankove, in *Hydrogen in Semiconductors,* edited by J. I. Pankove and N. M. Johnson, Semiconductors and Semimetals Vol. 34 (Academic, London, 1991), p. 47.
[27] R. G. Wilson, Appl. Phys. Lett. **49**, 1375 (1986).
[28] K. Irmscher, H. Hlose, and H. Maas, J. Phys. C **17**, 6317 (1984).
[29] A. Henry, O. O. Awaldelkarim, J. L. Lindström, and G. S. Oehrlein, J. Appl. Phys. **66**, 5388 (1989).
[30] A. Henry, O. O. Awaldelkarim, C. Hallin, J. L. Lindström, and G. S. Oehrlein, J. Electrochem. Soc. **138**, 1456 (1991).
[31] M. W. Hüppi, J. Appl. Phys. **68**, 2702 (1990).
[32] V. A. Singh, C. Weigwl, J. W. Corbett, and L. M. Roth, Phys. Status Solidi B **81**, 637 (1977).
[33] J. Bernholc, N. O. Lipari, S. T. Pantelides, and M. Scheffler, Phys. Rev. B **26**, 5706 (1982).
[34] G. G. DeLeo, W. B. Fowler, and G. D. Watkins, Phys. Rev. B **29**, 1819 (1984).
[35] G. L. Gutsev and G. S. Myakenkaya, Phys. Status. Solidi B **156**, 319 (1989).
[36] P. M. Mooney, L. J. Cheng, M. Süli, J. D. Gerson, and J. W. Corbett, Phys. Rev. B **15**, 3836 (1977).
[37] J. I. Pankove, in *Hydrogen in Semiconductors* (Ref. 26), p. 94.